aerospace

MDPI

Article

Throughput and Capacity Analysis of a Vertiport with Taxing and Parking Levels

Samiksha Rajkumar Nagrare * and Teemu Joonas Lieb

Institute of Flight Guidance, German Aerospace Center (DLR), Lilienthalplatz 7, 38108 Braunschweig, Germany
* Correspondence: samiksha.nagrare@dlr.de

Abstract

Amidst the increasing aerial traffic and road traffic congestion, Urban Air Mobility (UAM) has emerged as a new mode of aerial transport offering less travel time and ease of portability. A critical factor in reducing travel time is the emerging electric Vertical Take-Off and Landing (eVTOL) vehicles, which require infrastructure such as vertiports to operate smoothly. However, the dynamics of vertiport operations, particularly the integration of battery charging facilities, remain relatively unexplored. This work aims to bridge this gap by delving into vertiport management by utilizing separate taxing and parking levels. The study also focuses on the time eVTOLs spend at the vertiport to anticipate potential delays. This factor helps optimise arrival and departure times via a scheduling strategy that accounts for hourly demand fluctuations. The simulation results, conducted with hourly demand, underscore the significant impact of battery charging on operational time while also highlighting the role of parking spots in augmenting capacity and facilitating more efficient scheduling.

Keywords: vertiport; urban air mobility; vertiport throughput; operations management

1. Introduction

Predictions indicate that by 2030, approximately sixty per cent of the global population will live in cities, a trend anticipated to exacerbate congestion within ground-based transportation networks [1]. Leveraging technological advancements, Urban air mobility emerges as a promising option to ease transportation in the future. The term UAM transpires a pioneering paradigm of air transportation characterized by the safe and sustainable movement of passengers and goods using small, highly automated aircraft at lower altitudes in urban and suburban areas [2].

Deliberations surrounding the scope of the UAM framework are currently underway, leading to the emergence of expanded terminology such as Advanced Air Mobility (AAM) [3] and Innovative Air Mobility (IAM) [4]. AAM is a relatively new form of intermodal transportation, often referred to in the United States, that could extend well beyond high-density urban centres, adopting the electric and hybrid aircraft to urban, suburban, and rural operations [5]. Furthermore, the term IAM has gained prominence in Europe, encompassing intra-urban and inter-regional transit transportation. Research suggests that while IAM holds the potential to reduce travel duration compared to traditional ground-based transportation significantly, its introduction may have a limited impact on the utilisation patterns of customers [6]. Nonetheless, projections forecast global demand of up to 5.5 million IAM vehicles by 2050, necessitating corresponding infrastructure investments in Take-Off and landing facilities, namely vertiports [7].

Check for updates

Academic Editor: Eri Itoh

Received: 24 December 2025
Revised: 16 January 2026
Accepted: 20 January 2026
Published: 22 January 2026

Copyright: © 2026 by the authors. Licensee MDPI, Basel, Switzerland. This article is an open access article distributed under the terms and conditions of the Creative Commons Attribution (CC BY) license.

The term vertiport originated several decades back and is primarily associated with landing sites for air taxi operations using helicopters, tilt-rotor aircraft, and Vertical Take-Off and Landing (VTOL) vehicles [8]. Vertiports are envisioned similarly to a helipad, with the difference being the anticipation of the demand for vertiports exceeding the helipad in the coming future [9]. In other words, vertiports are dedicated areas that provide the infrastructure needed for safe commercial air transport by Vertical Take-Off and Landing Capable Vehicles (VCA) [10]. As IAM gains prominence, global efforts are underway to establish regulatory frameworks for vertiport operations. Notably, the European Union Aviation Safety Agency (EASA) has introduced regulatory provisions such as the special condition SC-VTOL-01 [11] and the Prototype Technical Specification (PTS-VPT-DSN) [12] for vertiports. In Europe, vertiports are often located within U-space areas, which are envisaged as digital ecosystems supporting Uncrewed Aircraft System (UAS) and IAM operations [13].

A critical aspect of vertiport design often revolves around its capacity to hold eVTOLs and its throughput, both factors intricately linked to cost-effectiveness. As outlined in [14], vertiport capacity is evaluated based on factors such as the number of landing pads, charging positions and parking bays. The maximum throughput is linked to the frequency of aircraft movements, that is, take-offs and landings within a designated time frame, typically measured per hour. Furthermore, vertiport operations encompass all activities and processes involved, including aircraft landings and Takeoffs, passenger boarding and disembarking, ground handling, and maintenance and security procedures. Current vertiport designs feature static vertipads for take-off and landing [15], requiring eVTOLs to hover for landing when the vertipads are busy. This problem can be addressed with an escalator-inspired taxing system, since time savings depend heavily on fast processing at the vertiports.

The current work dictates one approach to study the throughput of the proposed vertiport design. It emphasises reducing eVTOL wait times, thereby maximising the number of vehicles landing and taking off from the vertiport and handling more passengers. The specific contributions of the work are as follows:

- Proposed a novel vertiport design with an eVTOL parking system on a different floor/level.
- A comprehensive solution for scheduling eVTOLs in a flowchart to allocate and utilise vertiport resources to free vertipads.
- Study the effect of charging times on the overall throughput of the vertiport operations.
- Monte Carlo simulations to find the vertiport capacity threshold.

The proposed vertiport design paves the way for expanding the concept of multiple levels within the facility, dedicated to specific services that would be present in an ideal vertiport.

The rest of the paper is structured as follows: Section 2 reviews the recent studies in the field. Section 3 elaborates on the research problem, while Section 4 explains various terms, operational flows, and the time delays expected during an eVTOL's stay at the vertiport. Section 5 presents an approach to optimise vertiport throughput through scheduling, and the simulation results are discussed in Section 6. Lastly, Section 7 concludes the paper.

2. Related Work

Systematic literature reviews have been conducted on IAM and vertiports, as evidenced by the work of [9,16–19]. The referenced studies in the literature overview the critical role of ground infrastructure components for the efficient operation of IAM. The smooth integration for efficient IAM operations relies on well-designed departure and arrival procedures, effective communication with other airspace users and quick on-ground vertiport

operations. The optimal layout of vertiports is essential for ensuring smooth, time-efficient operations and minimising potential risks associated with increased air traffic in urban areas [9]. Furthermore, despite advances in understanding infrastructure needs, significant gaps remain in understanding regulatory frameworks, certification processes, and public acceptance of these emerging technologies [6].

In recent years, focus has been on integrating IAM and vertiport concepts into U-space and partially existing Air Traffic Management (ATM) environments, on-demand and dynamic capacity management services, and vertiport capacity and throughput enhancements. For example, ref. [20] provides an overview of air traffic management solutions for IAM, and ref. [21] investigated the successful integration of vertiport management tasks using a vertiport manager within the European UTM system, U-space. The findings show that in the first implementation phase, a human operator is required to approve or cancel air taxi operations. In addition, authors in [22] developed an innovative performance-measuring matrix specifically tailored to assess the operational efficiency of airborne traffic flow at vertiports and, as a result, facilitate strategic flight planning. However, these works do not specifically address ground-based operations at vertiports or tackle time-efficient vertiport concepts. On the other hand, authors in [23] investigated the impact of IAM vehicle design, regulation, and operation on the throughput capacity of vertiports, but did not emphasise the battery charging time or its effect on the overall vertiport operation time.

Guerreiro et al. in [19] proposed a vertiport scheduling algorithm on a first-come, first-served basis, highlighting that this approach can lead to inefficiencies in the use of the vertiport resources. Nevertheless, they analysed various vertiport configurations with varying parking and vertipad spacing limits at ground level, without considering different take-off, landing, and charging floors. In addition, the patent [24] proposes a concept of a multi-level fulfilment centre in which smaller UAS take off and land from several levels of one building. This fulfilment centre may have multiple levels or floors to accommodate parallel UAS operations, saving time and space required to operate numerous UAS. However, the authors did not foresee the utilisation of elevators to move the UAS between parking levels and battery charging positions.

In [25], the vertiport capacity was analytically estimated by considering the number and layout of take-off and landing spots, taxiways, gates, and parking positions, since these factors have a significant impact on vertiport throughput capacity and must be carefully designed, especially in space-constrained inner-city locations. In a similar direction, ref. [26] analysed a method for identifying suitable areas for vertiport infrastructure, given the already heavily congested urban areas in metropolitan regions. Using the developed vertiport selection method, city planners and other users can easily select a potential vertiport location on a city map and create a concrete vertiport layout with the ideal composition of vertiport elements, thereby easing future planning for vertiports by related authorities. Specific focus on the requirements for batteries used in IAM vehicles is given in [27], highlighting the need for fast-charging points at vertiports to ensure high throughput and short turnaround times.

Finally, several European research projects addressed integrating new airspace users and required infrastructure elements within U-space and existing airspaces. Within the CORUS-XUAM project [28], a concept of operations for U-space participants was developed, including IAM and vertiport operations, highlighting the need for harmonised procedures at vertiports. Moreover, recent EUREKA projects are developing U-space services to address the needs and requirements of vertiport concepts, enabling safe and efficient IAM operations in the future [29]. However, these projects do not address the characteristics of different vertiport configurations, nor the time-saving effects of battery charging bays

across different vertiport levels or innovative elevator concepts. Hence, a research gap was identified among the recent works.

3. Problem Statement

Managing vertiport operations, particularly the arrival, departure, and maintenance of eVTOL aircraft, poses a significant challenge for UAM systems. An essential aspect of this challenge is ensuring smooth transitions between vertiport functions, including Take-Off, landing, parking, charging, and repairs, all while minimising delays and maximising the use of available resources.

Figure 1 presents a schematic of the proposed multi-level vertiport system. The concept involves utilising multiple levels or floors of a vertiport building, specifically a taxi level and a parking level, which serve individual functions. The taxi level is designed for take-off, landing, and passenger entry/exit, while a parking level is provided for eVTOL parking in the event of a delay and battery charging. These two levels work in tandem to streamline vertiport operations. The taxi level handles high-traffic functions, such as vehicle arrival and departure, while the parking level supports maintenance and charging without interfering with critical operations.

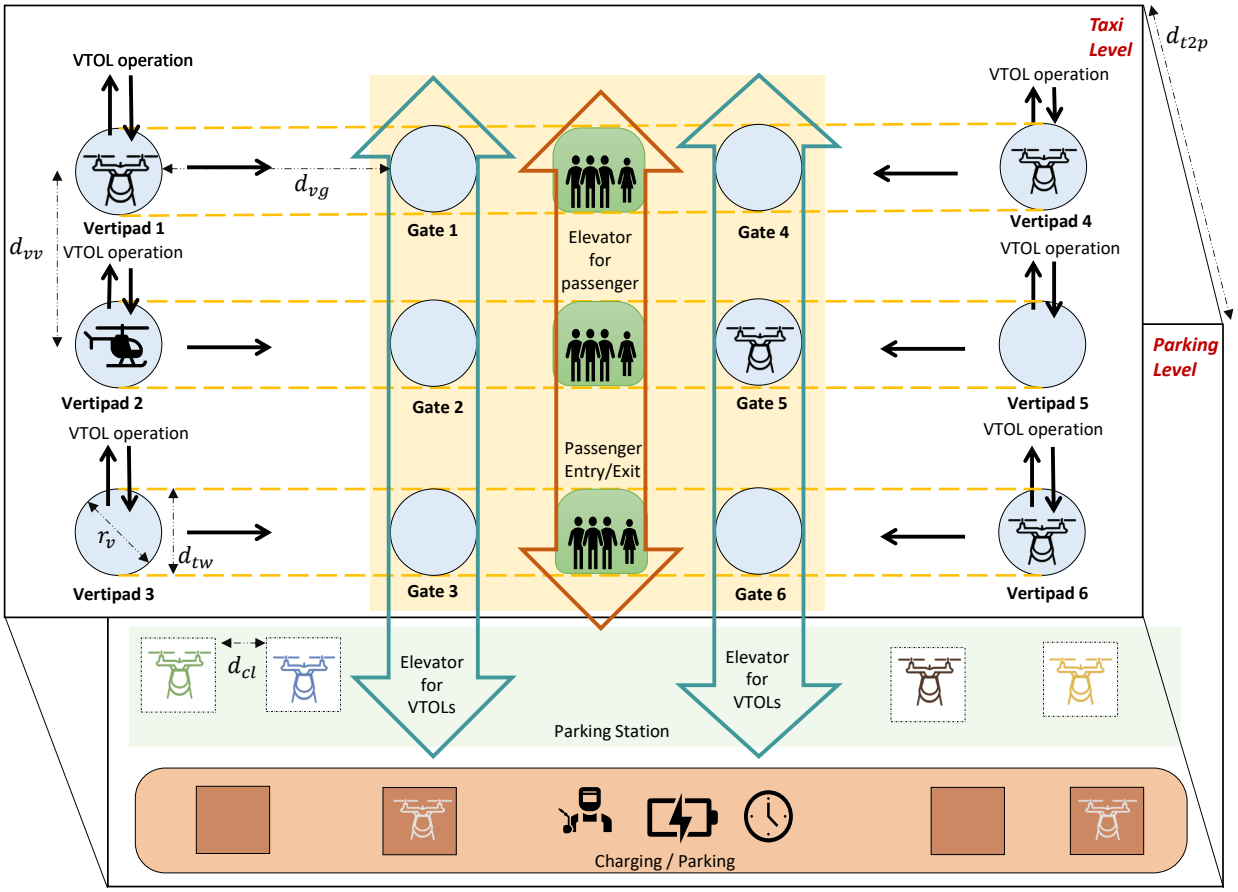

Figure 1. Proposed vertiport design with taxi and parking levels.

Key to the design are two types of elevators: a vehicle elevator for transporting eVTOLs between levels, located near the gates where passengers board and deboard, and a passenger elevator for moving passengers. This dual-elevator system enables quick cycling of eVTOLs in and out of the vertiport. Furthermore, using these two levels allows vertipads in vertiports to accommodate the next set of eVTOLs with minimal time delay, thereby improving vertiport efficiency in handling high traffic volumes.

This multi-level vertiport design is intended as a practical extension of operationally feasible emerging vertiport concepts. Structurally, it is designed to support loads similar to those of multi-story parking facilities and rooftop heliports [30], accommodating the weight of eVTOLs, vehicle elevators, and charging infrastructure. From a regulatory standpoint, the layout adheres to current vertiport guidelines, which focus on segregated operational zones, controlled passenger access, and safety redundancy, although detailed certification standards for multi-level vertiports are still evolving.

A two-level configuration was selected to balance operational efficiency and design complexity. Separating high-frequency functions, such as Take-Off, landing, and passenger exchange, from time-intensive activities, including parking and battery charging, reduces vertipad occupancy and improves throughput. Additional levels could further increase capacity but would introduce diminishing returns due to increased elevator transit times, higher construction costs, and greater regulatory complexity. Hence, this design is most applicable to medium- and large-scale urban areas with high-demand air mobility use cases for rapid transportation, equipped with infrastructure capable of supporting multiple levels.

To maximise the effectiveness of this design, this study aims to address the challenge of efficiently managing the scheduling and allocation of eVTOLs across vertiport functions, particularly in relation to the arrival and departure of eVTOL aircraft, while minimising operational downtime. With our proposed vertiport design, we aim to optimally allocate eVTOLs to vertipads, gates, battery charging stations, and parking spots, thereby fully utilising the vertiport's capacity while meeting all arrival and departure demands. Additionally, we intend to determine the duration of eVTOL presence at the vertiport and adjust operations accordingly, while also monitoring any associated delays. Our approach will ensure that vertiport resources are fully utilised, reducing eVTOL dwell time at the facility and enhancing overall system throughput.

4. Vertiport Elements

This section outlines the basic structure of the vertiport and introduces all the variables necessary to address the problem statement. The aim is to explain how the vertiport operates and define the key factors involved in solving the identified issues. This framework serves as a foundation for analysing and improving vertiport operations in a systematic manner.

4.1. Vertiport Design Considering Vehicle Dimensions

Figure 1 shows the configuration of the proposed vertiport, which has a total capacity of 20 spots. The layout features six active landing/Take-Off vertipads, six gates, and eight designated charging and parking areas. Additionally, two elevators are designated for eVTOL access on both levels, while a separate elevator is available for passengers.

In compliance with the EASA prototype guidelines [12], the design and layout of vertiports are carefully planned to ensure safety and efficiency in air mobility. For instance, the distance between two vertipads, d_{vv}, is maintained at 60 m for eVTOLs with a Maximum Take-Off Weight (MTOW) of 3175 kg, adhering to the required clearances. As for the distance between the gate and a vertipad, d_{vg}, it is kept at 60 m for simplicity. Thereby, we selected four different eVTOL aircraft for this vertiport, as given in Table 1. It details their dimensions, battery capacities and seating capacities.

We define D as the diameter of the smallest circle in meters that contains the projection of the largest eVTOL aircraft the vertiport is intended to serve on a horizontal plane during Take-Off or landing, considering the rotors are in motion. For the maximum tip-to-tip span of 9.2 m of the expected eVTOLs at the vertiport as given in Table 1, we consider $D = 10$.

Consequently, the vertiport diameter must have a 25% clearance according to the EASA guidelines [12]. That is, $r_v = 1.25D$. Similarly, the minimum distance between taxiways, d_{tw}, must have 50% clearance. Finally, in the eVTOL parking mode, the distance between two vehicles, d_{cl}, is maintained at a minimum of 3 m.

Table 1. Vehicle characteristics of different eVTOLs.

eVTOL	Tip-to-Tip Span (m)	Total Seats	MTOW (kg)	Battery Capacity (kWh)
Vahana	5.7	3	815	38
eHang 216	5.61	2	620	17
CityAirbus	8	5	1600	110
Volocopter 2X	9.2	2	450	100

4.2. Vehicle Operation Flow Through the Vertiport

Figure 2 illustrates a typical journey undertaken by an eVTOL aircraft, spanning from its arrival at the vertiport to its departure. Upon arrival at the designated vertipad, the aircraft taxis to the gate to facilitate passenger disembarkation. It is worth noting that eVTOL operations are subject to following the respective taxiways that connect vertipads and gates (shown in dotted lines in Figure 1). Therefore, operations at any vertipad would result in the corresponding landing at either gate on its taxiway. For example, eVTOLs landed at vertipad 1 would allow passenger de/boarding at gate 1. If gate 1 is busy, the eVTOL will continue towards gate 4, which is also on its taxiway. However, eVTOLs approaching vertipad 1 would not go to gates 2, 3, 5 and 6.

Figure 2. A typical eVTOL journey through the vertiport.

Once the eVTOL arrives at the gate, it undergoes a series of checks, including assessing its battery level and identifying potential repair needs. If the eVTOL requires a substantial amount of battery, which was expended on its last trip, it is directed to a charging centre. Then, based on its scheduled departure time, a decision is made whether to retain the eVTOL at the parking level or return it to the boarding gate and then to the vertipad for take-off.

To ensure a timely departure, the eVTOL is typically required to be at the vertipad a few minutes before its scheduled Take-Off time. This buffer allows for passenger boarding, engine start-up procedures, and the loading of the planned route. Finally, the eVTOL taxis back to the vertipad from the gate and takes off. It is important to note that a vertipad remains occupied until both the landing and take-off times have elapsed.

4.3. Turnaround Times for Operations

In the context of the current work, specific fluctuations in operational procedures may result in delays due to varied vertiport processes, services, and resource occupancy durations (gates, vertipads, and charging spots). In a typical eVTOL journey shown in Figure 2, it is interesting to see the amount of time an eVTOL spends at a vertiport, commonly referred to as the turnaround time ($T_{\text{turnaround}}$), and is given as follows:

$$T_{\text{turnaround}} = 2t_{\text{tol}} + 2t_{\text{sse}} + 2t_{\text{pbd}} + 2t_{\text{taxi}} + t_{bc} + t_{clear} + t_{\text{ele}} + t_r. \quad (1)$$

Here, the time taken by eVTOL to land and take off upon arriving at the vertiport is t_{tol}. The boarding and disembarking process duration is denoted by t_{pbd}, and the time required to travel from a vertipad to the gate is t_{taxi}. Gate operations may involve uncertainties due to human involvement and terminal procedures. Furthermore, the time to charge the batteries is denoted by t_{bc}, and the available charging power at the vertiport is η. Additionally, because the eVTOL vehicle charging is located on the parking level, the time spent in the elevator (t_{ele}) adds to the total time. Likewise, the time for repairs (t_r) can be accounted for, varying with the severity of the vehicle's condition, ranging from quick fixes to more extensive repairs. Moreover, departure and Take-Off delays may stem from pending clearances and the non-availability of vertipads. These time delays are represented with t_{clear}. The start and stop engine times t_{sse} are also considered to cover all the bases.

Equation (1) represents the cumulative turnaround time caused by all the aforementioned factors, including delays, in transitioning an eVTOL from landing to Take-Off. In this equation, the terms $t_{\text{tol}}, t_{\text{sse}}, t_{\text{pbd}}$ and t_{taxi} are each multiplied by a factor of 2. This is because it is assumed that for every eVTOL that lands at the vertiport, there is a corresponding Take-Off, and thus each event (landing, Take-Off, starting engine, stopping engine, passenger boarding, passenger deboarding, and taxiing) must be calculated separately for both phases. In the ideal turnaround scenario, Equation (1) reduces to Equation (2), eliminating all delays, including eVTOL charging. Here, the ideal turnaround time is represented by T_{ideal} and can be calculated as follows:

$$T_{\text{ideal}} = 2t_{\text{tol}} + 2t_{\text{sse}} + 2t_{\text{pbd}} + 2t_{\text{taxi}}. \tag{2}$$

In simpler terms, T_{ideal} is the ideal time an eVTOL spends on the vertiport. In this scenario, the battery level of the eVTOL is calculated to be sufficient for its next trip, including a battery reserve. It is also valid in this case that the resources (vertipad, gates) are available at the specific time instances an eVTOL needs them.

Other delays that may arise include the time discrepancies between the passenger's trip request and the air taxi's boarding availability. Moreover, security screenings may introduce additional time requirements influenced by varying traffic conditions across different hours, days, and seasons. Upon reaching the designated gate, the passenger boards while the air taxi undergoes preparation for departure. Decisions regarding the duration of passenger waiting times and booking reservation expirations have a significant impact on deadhead flights, although this is outside the scope of the current work.

4.4. Battery Charging Time

In analysing eVTOL aircraft operations, understanding energy consumption and battery usage is vital. It helps determine the time needed to recharge the battery, which is crucial for efficient operations management. This subsection elaborates on the variables involved in the vertiport scenario and discusses their significance. Let M represent the mass of the eVTOL in kg, which is needed to calculate the energy required for an eVTOL flight. Let X_t denote the distance travelled by the eVTOL, where X_{pt} represents the distance covered in its previous trip, and X_{nt} corresponds to the upcoming scheduled trip. Both distances are measured in kilometres (km).

Let the specific energy consumed by the eVTOL in its previous trip, denoted as S_{pt} in Wh/kg, and the battery capacity of an eVTOL is represented by B_{cap} in kWh. Now, to describe the relationship between X_{pt} and S_{pt}, we derive Equation (3) by analysing the linear relationships between specific energy and the distance travelled by the vehicle as seen in [27], assuming a lift-to-drag ratio of 9 units. In this equation, $\mathcal{K}$ denotes the slope of the linear relation, measured in km/Wh/kg.

$$X_t = \mathcal{K}S_t = 1.5S_t \tag{3}$$

Assuming the energy available from the battery is E_{init} kWh, and the energy consumed during the previous trip is E_{cons} kWh, then the energy remaining after the trip is $E_{rem} = E_{init} - E_{cons}$, in kWh. To initialise, we assume $E_{init} = B_{cap}$, whereas the E_{cons} is the product of the specific energy consumption rate and the mass of the eVTOL, as seen in Equation (4). In terms of the distance travelled in the previous trip, as given in Equation (5), the value of S_t is compared from Equations (3) and (4).

$$E_{cons} = MS_t \times 10^{-3} \tag{4}$$

$$\text{Using Equations (3) and (4)}, \quad E_{cons} = \frac{MX_t}{1500} \tag{5}$$

Finally, the percentage of battery remaining after the trip, denoted as $\%B_{rem}$, is calculated as the ratio of the remaining energy by the initial energy, as shown in Equation (6). It provides an integral indicator of the eVTOL's battery status post-flight, with charging power at the vertiport parking level set to η kW. The final charging time, t_{bc}, needed to fully charge the remaining battery is calculated using Equation (7) and measured in minutes.

$$\%B_{rem} = \frac{E_{rem}}{E_{init}} \times 100 = \frac{E_{init} - E_{cons}}{E_{init}} \times 100 = \left(1 - \frac{MX_t}{1500B_{cap}}\right) \times 100 \tag{6}$$

$$t_{bc} = \frac{B_{cap}}{\eta}\left(1 - \frac{\%B_{rem}}{100}\right) \times 60 \tag{7}$$

On the other hand, it is also possible to charge the eVTOL with a minimum amount of battery required, based on its X_{nt}, to ensure the vehicle has enough energy to complete the upcoming trip. It is considered safe to maintain a 20% reserve battery for an eVTOL before undertaking its journey, as suggested in [31]. This not only ensures the eVTOL has sufficient energy for the upcoming trip but also quickly frees up charging slots, creating space for other eVTOLs and improving the vertiport's throughput. Additionally, maintaining a 20% reserve provides an extra safety margin in the event of unexpected changes in flight conditions or delays. Hence, the charging duration in the current work is defined as the time required to achieve this minimum reserve.

There are a few tradeoffs for partially charging an eVTOL. It enables faster turnarounds and reduced peak power and infrastructure requirements, but tightens operational margins by leaving less energy buffer for contingencies such as rerouting or delays and increasing reliance on precise scheduling. While each charge event is shorter and lower in energy, the resulting throughput increases system complexity and demands more advanced power management and coordination. Although improved utilisation can boost revenue, these gains may be partially offset by higher integration, monitoring, and maintenance costs. Consideration of the tradeoff mentioned above is beyond the scope of the current work.

5. Solution Approach

This section describes the solution approach towards the problem of optimising the vertiport throughput using the vertiport elements described in the previous section.

Suppose the vertiport experiences an hourly eVTOL arrival demand of $N^{A/h}$ and an hourly eVTOL departure demand of $N^{D/h}$. Let $T^{A/h} = \{T_i^{A/h} | i = 1, 2, \ldots, N^{A/h}\}$ represent the desired arrival times of eVTOLs at the vertiport per hour, and $T^{D/h} = \{T_j^{D/h} | j = 1, 2, \ldots, N^{D/h}\}$ denote the desired departure times of eVTOLs at the vertiport per hour. Here, the indices i and j represent any k^{th} eVTOL arriving and departing

at the vertiport, respectively. The total demand per hour is given by $N^{S/h}$, calculated as $N^{S/h} = N^{A/h} + N^{D/h}$. The set indicating the arrival and departure eVTOL demands is given as follows:

$$T^{S/h} = T^{A/h} \cup T^{D/h} = \{T_k^{S/h} | k = 1, 2, \ldots, N^{S/h}\}. \quad (8)$$

The schematic flowchart shown in Figure 3 depicts the solution for accommodating the total hourly demand. To initiate the scheduling algorithm, specific inputs are required, including arrival or demand requests to the vertiports, the occupancy status of each vertipad, gate, and charging/parking station. Initially, the desired arrival and departure times of eVTOLs are organised in ascending order to determine the time at which the vertipads need to be available.

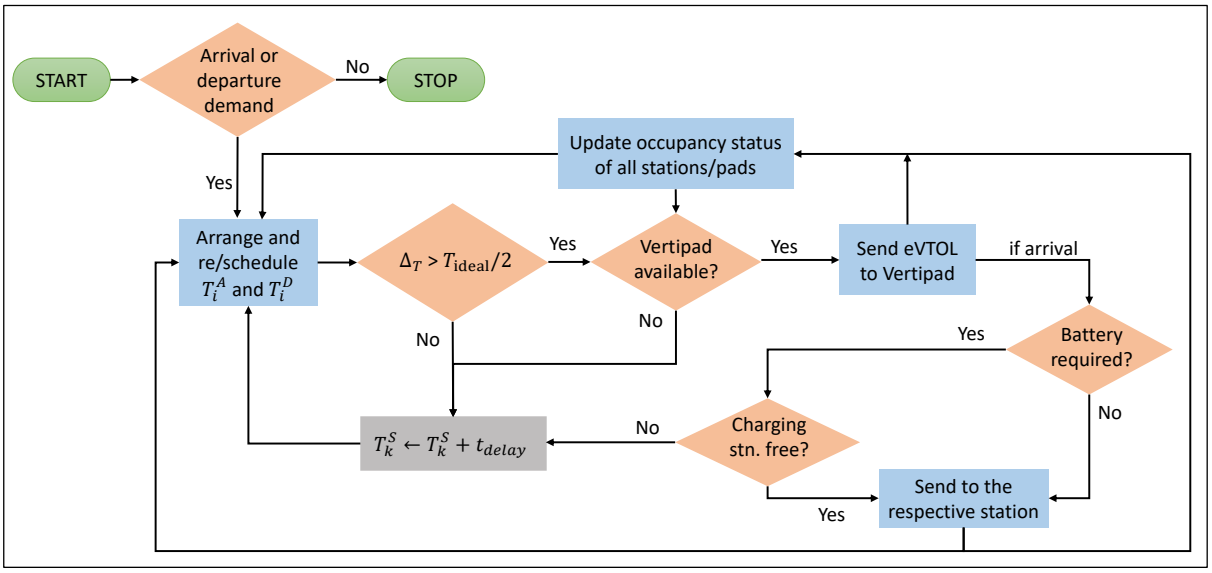

Figure 3. Flowchart depicting the resource utilisation planning to maximize throughput process.

It is assumed that the vertipad is considered busy from the moment the eVTOL begins hovering until it lands on the vertipad and continues until the eVTOL taxis to the gate and passengers deboard. Therefore, to ensure safe distances between two eVTOLs on the taxiway, the difference between the arrival/departure times between two eVTOLs (say k and $k+1$) must be Δ_T. In other words, $\Delta_T = T_{k+1}^{S/h} - T_k^{S/h} > T_{\text{ideal}}/2$. If this condition is met, no scheduling is required for eVTOLs to land or take off from vertipads. However, scheduling may still be necessary to optimise the use of charging stations.

When it comes to charging slots, they are considered occupied if an eVTOL is redirected to the charging station, should it require charging to undertake its next scheduled trip. The charging stations are at the parking level, which adds an extra elevator travel time, t_{ele}. If an eVTOL reaches the charging station but all stations are occupied, the vehicle is expected to wait at the gate until its turn to charge. Alternatively, if the charging station is free, the eVTOL is charged and then returned to the vertipad. Throughout these processes, the occupancy status of all stations is updated.

If a vertipad is unavailable for a departing eVTOL, a delay (t_{delay}) is added to the departure time, and its availability is rechecked. However, for an eVTOL approaching for arrival, if the distance between its previously scheduled eVTOL and the next scheduled eVTOL meets the minimum desired time, but if all vertipads are busy, then the vehicle is either redirected to another nearby vertiport or a delay could be added to its arrival time. However, the latter option may create a chain reaction and affect subsequent scheduled

eVTOLs. In such cases, one workaround is to fill the vertiport near capacity by accommodating eVTOLs in any available station, preferably parking stations, to accommodate incoming vehicles. The algorithm concludes when all arrival and departure demands have been met. In this work, we assume no dwell time for incoming eVTOLs when no vertipads are available. In other words, if a vertipad is not available when an eVTOL wants to land, it is redirected to another vertiport.

6. Simulation Results

A set of simulations was conducted to evaluate vertiport throughput using a combined Discrete Event Simulation (DES) and Monte Carlo methods to capture both the operational logic of vertiport processes and the stochastic nature of demand and service times. DES is employed to model the sequence of discrete operational events, including eVTOL arrivals, landings, ground handling, charging, and departure, where system states change only at specific event times. Whereas Monte Carlo sampling incorporates stochastic variability in arrival patterns, arrival battery percentages, and service times, enabling a statistically robust performance assessment.

The baseline scenario was tested with 475 eVTOL arrivals over a 24-h period. An adaptability analysis is then performed by increasing demand from 50 to 50,000 eVTOLs per day to identify vertiport capacity limits and the effects of congestion on resources. Furthermore, key metrics for evaluating vertiport throughput are defined and analysed across all scenarios.

6.1. Simulation Parameters and Data

Simulations are performed for 4 different eVTOLs, the data for which are given in Table 1, and the results are tested via a DES in MATLAB 2023b. The time was discretised in minutes for every hour of the day. Computations are carried out on a 13th-generation Intel(R) Core(TM) 64-bit operating system with an i7 processor, 16 GB of RAM, and a base clock speed of 1.90 GHz.

In the vertiport setup depicted in Figure 1, we have 6 vertipads available for take-off and landing, 6 gates for passenger boarding and deboarding and two elevators for transfer to the parking level, along with 8 charging stations and parking spots. Therefore, the vertiport can accommodate up to 20 eVTOLs simultaneously. To evaluate the effectiveness of the proposed method, random arrival demands were generated for a typical day. Table 2 summarises the key variables and their corresponding values used in the simulation.

The range of distances travelled by the specific eVTOLs from Table 1 was selected to stay between [14, 56] km for Vahana, [9, 34] km for eHang 216, [21, 83] km for City Airbus, and [67, 267] km for Volocopter. The selected ranges are designed to account for a 20% energy reserve required for safe operations, as recommended in [31]. This means that the specified distances already include a margin, ensuring the vehicle has at least 20% battery remaining after completing the longest trip within its range.

Table 2. Variables used in the simulations

Sr. No.	Variable	Description	Value	Units
1	t_{bc}	Battery charging time	Equation (7)	min
2	t_{pbd}	Passenger de/boarding	90	s
3	t_{tol}	Take-Off/landing time	2	min
4	t_{sse}	Engine start/stop	30	s
5	V_{ee}	Elevator speed	0.3	m/s
6	d_{vv}	Vertipad to vertipad distance	60	m
7	d_{t2p}	Distance between taxing and parking levels	10	m
8	d_{cl}	Parking clearance	3	m
9	d_{vg}	Distance between vertipad and gate	30	m
10	η	Charge power	100	kW

6.2. Metrics for Throughput Analysis

1. Aircraft redirected ($N_{redirected}$): It gives the total number of eVTOLs redirected in a day when no vertipad was available for their landing at the scheduled arrival time.
2. Number of eVTOL served ($\mathcal{N}_{eVTOL}$): It calculates the total number of eVTOLs that were handled within a period of time (day or hour) by the vertiport.
3. Service rate (%$\mathcal{S}$): This metric evaluates the percentage of eVTOLs landed, or that were served at the vertiport in a day, to the number of actual arrival demand for that day. Equation (9) represents it mathematically, where N^A is the total arrival demand for a day. Here, only the arrival demand is considered because eVTOLs departing from the vertiport cannot be redirected since they are already at the vertiport.

$$\%\mathcal{S} = \frac{N^A - N_{redirected}}{N^A} \times 100 \tag{9}$$

4. Average delays ($\mu_{avg/ev}$): It evaluates the average delays faced by each eVTOL per hour ($\mu^h_{avg/ev}$) or average delay faced by an eVTOL per day ($\mu^{day}_{avg/ev}$).
5. Arrival throughput ($\mathcal{A}^T$): It indicates how many eVTOLs can be successfully accommodated for landing compared to the total number of eVTOLs requesting landing within the same period. A higher arrival throughput suggests a more efficient system for handling incoming traffic. The notation is modified to $\mathcal{A}^T$/h when calculated hourly and to $\mathcal{A}^T$/day when calculated daily.
6. Departure throughput ($\mathcal{D}^T$): The departure throughput is the ratio of actual departures to the actual demand. It reflects how many eVTOLs can depart within a given period relative to the number that requested to depart. A higher departure throughput indicates that the system can efficiently handle outbound traffic. The notation is modified to $\mathcal{D}^T$/h when calculated hourly and to $\mathcal{D}^T$/day when calculated daily.
7. Overall throughput ($\mathcal{O}^T$): Overall throughput is the ratio of actual arrivals and departures to the total demand (arrivals and departures). If calculated each hour, it is $\mathcal{O}^T$/h, and if calculated per day, it is $\mathcal{O}^T$/day.

6.3. Representation of Demand of 475 eVTOL Scenario

In this subsection, we consider the vertiport configuration shown in Figure 1 and aim to accommodate eVTOLs over a 24-h period. Figure 4 provides a detailed overview of hourly vertiport demand, comparing expected demand with the actual number of eVTOLs accommodated. The total vertiport demand is represented as $\sum_h N^{S/h} = 949$, with $\sum_h N^{A/h} = 475$ eVTOLs being arrival requests to the vertiport, and $\sum_h N^{D/h} = 474$ eVTOLs requesting departures. Although the total demand includes both arrival and departure requests, the total number of eVTOLs to be accommodated remains 475. This is because we assume that there are zero eVTOLs at the vertiport at the start of the simulation,

and the eVTOLs that land on the vertiport are ideally scheduled to depart, assuming they have an ideal turnaround time (T_{ideal}).

Specifically, the arrival demands for each hour are $T^{A/h}_{demand}$ = [30, 25, 15, 30, 20, 15, 40, 35, 20, 25, 25, 10, 10, 20, 10, 35, 10, 10, 5, 10, 15, 10, 35, 15], and the actual arrivals are $T^{A/h}_{actual}$ = [30, 24, 16, 30, 19, 16, 40, 34, 21, 24, 26, 10, 10, 20, 10, 34, 11, 10, 5, 9, 16, 10, 35, 15]. Similarly, the ideal departures for each hour are $T^{D/h}_{ideal}$ = [28, 24, 17, 27, 22, 17, 35, 34, 23, 22, 29, 11, 11, 19, 10, 30, 13, 12, 3, 11, 14, 12, 30, 20] and the actual departures are $T^{D/h}_{actual}$ = [22, 29, 9, 32, 24, 15, 33, 31, 28, 21, 25, 17, 11, 17, 13, 21, 21, 13, 5, 8, 13, 15, 28, 22]. Each eVTOL is assigned an ID on a first-come, first-served basis. We assign IDs to eVTOLs that have been redirected to ensure redirection is accounted for. In this case, a total of three eVTOLs were redirected ($N_{redirected} = 3$), with two arriving at 07:00 and one at 16:00. Therefore, the total number of eVTOLs served was $N_{eVTOL} = 473$.

When examining the comparison between desired and actual arrivals and departures in more detail, it is evident from Figure 4 that a discrepancy exists between the demand and actual data. For instance, at 16:00, the actual number of arrivals is 35 eVTOLs, compared to the scheduled 34. The extra eVTOL from the previous hour arrived during this hour. Furthermore, one eVTOL (ID = 346) was redirected since all vertipads were occupied at its arrival time of $T^{A/h}_{346} = 925$ min. Similarly, in the case of departing eVTOLs, of the scheduled 30, only 21 could depart at 16:00. The remaining departures are transferred in the subsequent hours.

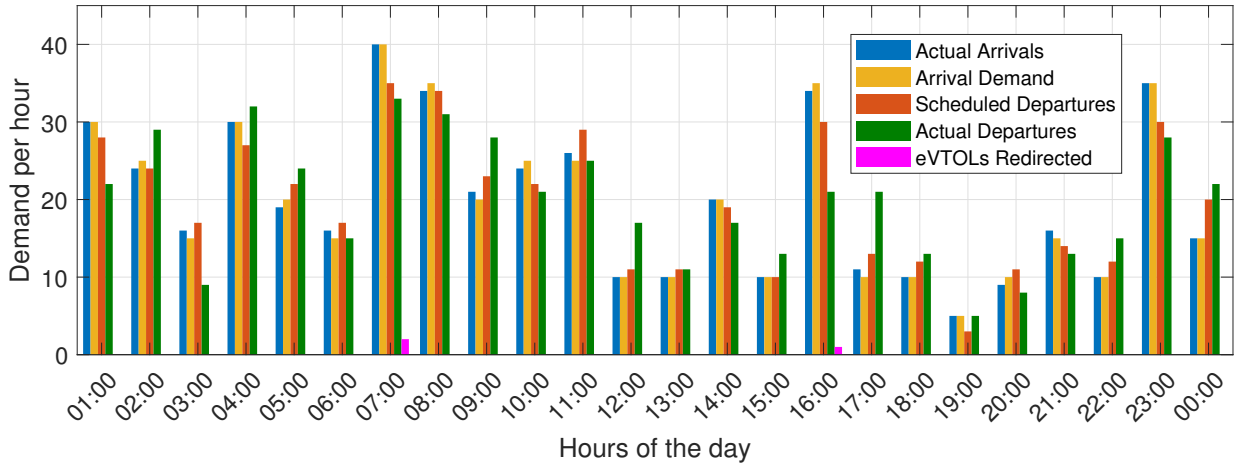

Figure 4. Vertiport demands generated per hour and actual demand fulfilled.

Utilising this data, we can determine the hourly arrival, departure and overall throughput of the vertipad. It can be seen in Figure 5. A throughput greater than 1 indicates that the vertiport is handling more operations than scheduled, while a throughput of less than 1 means the vertiport resources are underutilised.

Accordingly, at 16:00, the arrival throughput $\mathcal{A}^T = 0.97$, which is slightly less than 1, as actual arrivals were fewer than demand, and the departure throughput at 16:00 is $\mathcal{D}^T = 0.7$. However, there are a few time intervals during which the departure throughput remains greater than 1. For instance, at 17:00, $\mathcal{D}^T = 1.61$, indicating the actual departures were 61% more than the scheduled departures.

The overall throughput for the vertiport with 475 eVTOLs is then $\mathcal{O}^T = 1.02$. It suggests that the proposed solution strategy can effectively accommodate and manage eVTOLs without causing significant delays, as arrival and departure demands match actual arrivals and departures throughout the day.

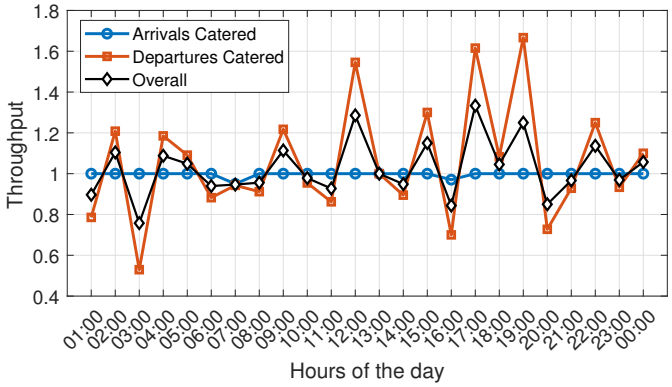

Figure 5. Vertiport throughput per hour.

In Figure 5, the arrival throughput is very close to 1, whereas the departure throughput fluctuates significantly. This is because the departure time is highly dependent on the time required to charge the battery, if necessary. Once the battery is charged, additional delays affect eVTOL departure scheduling. Furthermore, other delays may also occur, such as t_{clear}, when all the vertipads are occupied, preventing an eVTOL from occupying a gate coming from the parking level to the taxi level. In this case, the eVTOL is kept parked at the parking level.

The occupancies of these resources are shown in Figure 6. Specifically, Figure 6a shows the occupancy of vertipads each hour of the day, measured in minutes. It can be seen that vertipad 1 is the busiest, followed by vertipads 2, 3, 4, 5, and 6 in ascending order of occupancy. This is because the vacancy of vertipads is checked in increasing order of vertipad ID. The same applies to Figure 6b, where the occupancy of gates is shown.

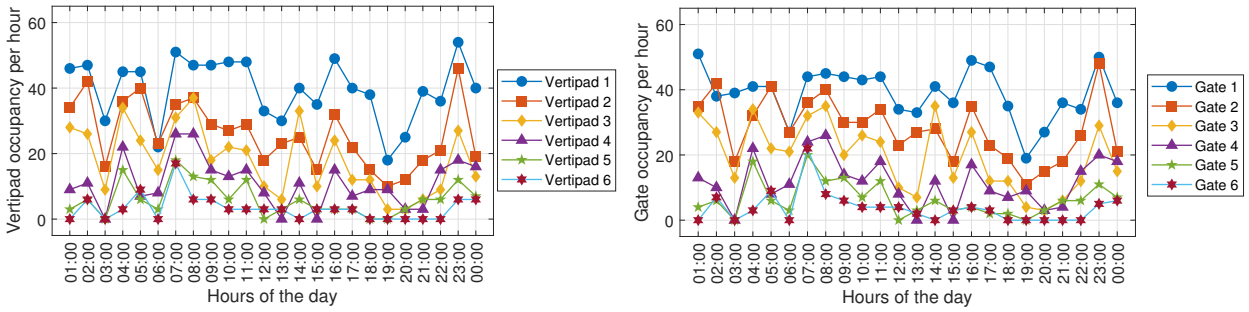

(**a**)

(**b**)

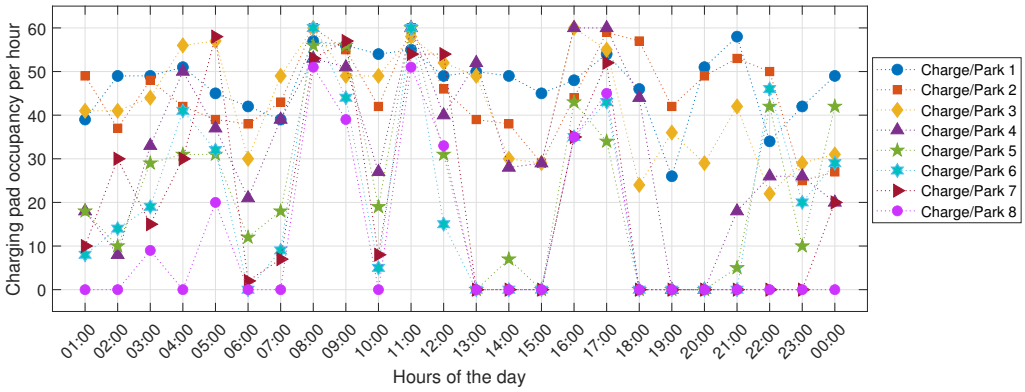

(**c**)

Figure 6. Vertiport occupancy status of the available resources for each hour of the day. Specifically, (**a**) the vertipad occupancy; (**b**) the gate occupancy and; (**c**) the charging and parking slot occupancy.

As mentioned earlier, eVTOLs always taxi from their occupied vertipad to the gates along their taxiway. eVTOLs can also move between gates. Figure 6c illustrates the occupancy status of 8 charging and parking spots every hour, measured in minutes. It is observed that the maximum value reached in Figure 6a–c is 60, corresponding to 60 min within an hour. For instance, at 16:00, covering the period from 1501 to 1600, vertipad 1 was occupied for 49 min, vertipad 2 for 32 min, vertipad 3 for 24 min, vertipad 4 for 14 min, and vertipads 5 and 6 for 3 min each.

As for gate occupancy at 16:00, Gate 1 is occupied for 49 min, Gate 2 for 35 min, Gate 3 for 27 min, Gate 4 for 17 min, and Gates 5 and 6 for 4 min each. Finally, regarding the charging and parking stations at 16:00, Station 1 was occupied for 48 min, Station 2 for 44 min, Stations 3 and 4 for the entire 60 min, Station 5 for 43 min, and Stations 6, 7, and 8 for 35 min each.

Accordingly, the total time spent by eVTOLs is given in Figure 7. The turnaround times for each eVTOL type vary due to delays in freeing vertipads for departure, as well as battery requirements and capacities. The figure indicates that the time spent by the eVTOL lies above the minimum turnaround time of T_{ideal}. Here, the ideal turnaround time is calculated as follows: $T_{ideal} = 2 \times (2 + 0.5 + 1.5 + 1) = 10$ min, calculated using Equation (2).

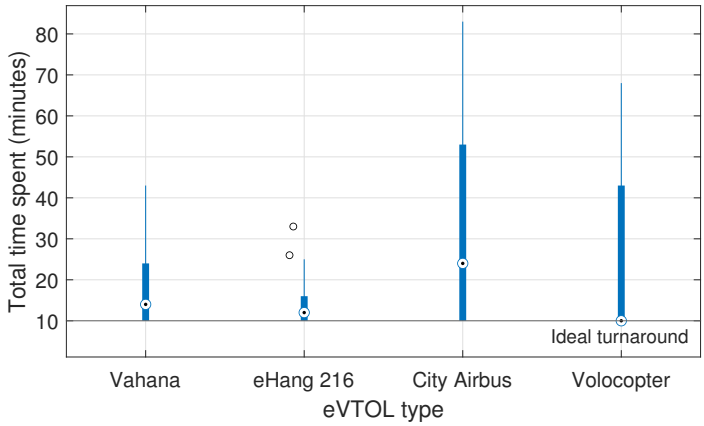

Figure 7. Turnaround times per eVTOL type.

The boxplot representing the time spent by eVTOLs includes five key elements for summarising this data. These elements include the minimum (0 percentile), the maximum (100 percentile), the median (50 percentile), and the first (25 percentile) and third quartiles (75 percentile). The rectangular strip in the boxplot indicates the range between the first and third quartiles. The circle within the rectangular strip with a dot at its centre represents the median value. Any circles located outside the extended lines are referred to as outliers. These extended lines beyond the rectangular strip are called whiskers. They represent the extremes of the data points, which are the whisker minimum and whisker maximum values, excluding any outliers [32]. Consider eHang 216 as an example. The plot shows a whisker minimum of 10 min, a whisker maximum of 33 min, a median of 12 min, a first quartile of 10 min, and a third quartile of 16 min, along with two outliers lying at 26 min and 33 min.

In this demand scenario shown in Figure 4, 231 eVTOLs that arrived at the vertiport were sent to charging stations. Among these, 61 were Vahana, 61 were eHang 216, 65 were City Airbus, and 45 were Volocopter. Their remaining battery level percentage upon arrival at the vertiport is shown in Figure 8a, and the required battery to complete their next trip is illustrated in Figure 8b. It can be seen that the distances travelled by the eVTOLs maintain a 20% reserve during eVTOL arrival and departure.

Delays faced by the eVTOLs are shown in Figure 9. When eVTOLs have an ideal turnaround time, delays at the vertiport are zero because they spend only the minimum time required to complete their mission and do not require charging assistance. It can be seen that the delays reach a maximum of 76 min for City Airbus (ID 358). This eVTOL arrived with a battery charge of 62.1%, and it required 75.6% for its next trip, which took 50 min to recharge. Furthermore, due to busy vertipads, the aircraft remained parked at the parking level for 15 min, and 1 min was spent in the elevator. Consequently, the average delay per hour throughout the 24-h period, including all eVTOLs serviced at the vertiport during their respective hours, is calculated to be $\mu^{day}_{avg/ev} = 9.62$ min.

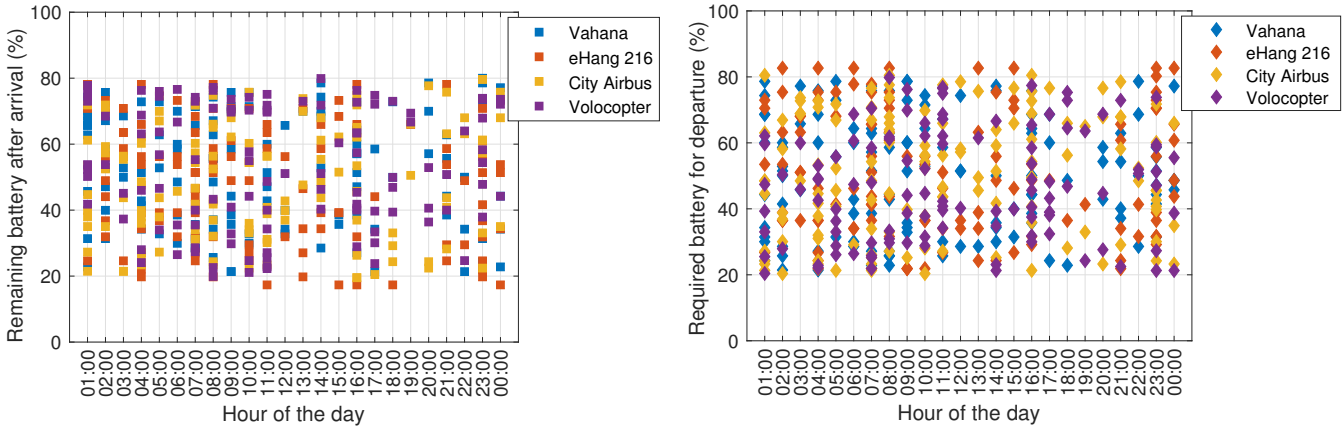

(**a**) (**b**)

Figure 8. Battery levels of all eVTOLs: (**a**) after arrival at the vertiport and (**b**) required for departing from the vertiport.

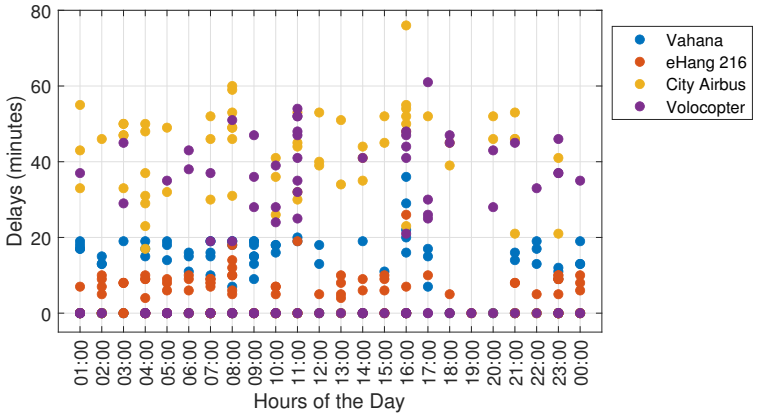

Figure 9. Delays faced by specific eVTOL types.

6.4. Throughput Results with Monte Carlo

The throughput of the vertiport was explored using Monte Carlo simulations with daily arrival demands ranging from 50 eVTOLs to 50,000 eVTOLs. The aim of this exercise is to determine the percentage of eVTOLs that can be served at the vertiport over a 24-h period and to find the vertiport's throughput capacity.

Table 3 provides an overview of the various arrival demands per day (Arrivals/day), the number of eVTOLs served at the vertiport ($\mathcal{N}_{eVTOL}$), the percentage of eVTOLs serviced at the vertiport (%$\mathcal{S}$), the average delay per hour over 100 iterations (μ^{h}_{avg}), the average number of eVTOLs redirected per day over 100 iterations ($N_{redirected}$/day), and the daily throughput of the vertiport, including arrivals ($\mathcal{A}_T$/day), departures ($\mathcal{D}_T$/day), and overall throughput ($\mathcal{O}_T$/day), all averaged over 100 iterations.

The data in the table were collected over 100 iterations across different arrival-time configurations, with various eVTOL types arriving at random intervals. Additionally, the remaining battery levels upon arrival at the vertiport were varied significantly. This was achieved by randomly selecting the distances X_{pt} and X_{nt} from predefined distance ranges for all eVTOLs, thereby accounting for different charging durations depending on the battery state.

This tabulated data can be visualised in Figure 10. Based on the data, the vertiport demonstrates a clear transition from high-efficiency operations to a state of total saturation. At low demand levels, the vertiport operates near perfection. With a service rate (%$\mathcal{S}$) of nearly 100% and negligible delays (μ^h_{avg}) under three minutes, the facility manages traffic without any aircraft redirections. In this phase, the overall throughput ($\mathcal{O}_T$) remains at approximately 0.99, indicating that the vertiport is currently under-utilised and it is equipped to handle the current traffic without any aircraft redirections.

Table 3. Monte Carlo simulations for high-density eVTOL operations at the vertiport (100 iterations).

Arrivals/Day	$\mathcal{N}_{\text{eVTOL}}$	%$\mathcal{S}$	μ^h_{avg}	$\mathcal{A}_T$/Day	$\mathcal{D}_T$/Day	$\mathcal{O}_T$/Day	$N_{redirected}$/Day
50	50	100	0.30 min	1	0.9950	0.9975	0
100	100	100	0.52 min	1	0.9866	0.9933	0
300	294.98	98.32	3.03 min	0.983	0.9824	0.9829	10
500	497.9	99.57	2.8 min	0.9958	0.9898	0.9928	2.12
700	679.44	97.06	3.61 min	0.9706	0.9846	0.9776	20.56
1000	943.99	94.39	4.9 min	0.944	0.9395	0.9417	56
1200	1014.4	84.53	5.33 min	0.8453	0.8958	0.8704	185.63
1500	1167	77.80	6.28 min	0.778	0.8519	0.8148	332.98
2000	1476.13	73.80	8.1 min	0.7381	0.7796	0.7588	523.87
2500	1625.58	65	9.42 min	0.6502	0.7486	0.6993	874.42
3000	1656.21	55.2	9.29 min	0.5521	0.7759	0.6637	1343.79
4000	1848.77	46.21	9.75 min	0.4622	0.7049	0.5855	2151.23
5000	1911.32	38.22	10.3 min	0.3823	0.7051	0.5432	3088.68
7500	1980.07	26.4	10.2 min	0.264	0.6934	0.4782	5519.93
10,000	2003.14	20	11.22 min	0.2	0.6934	0.4458	7996.86
12,500	2014.9	16.11	22.79 min	0.1612	0.6879	0.4238	10,485.14
50,000	2018.6	4.04	43.05 min	0.04	0.698	0.3682	47,981.4

The vertiport reaches its most efficient balance between 500 and 1000 arrivals per day. In this range, the facility maintains an overall throughput above 0.94 and average delays below 5 minutes. This performance aligns with the vertiport standard for the peak throughput-to-capacity ratio benchmark [19]. While redirected aircraft ($N_{redirected}$) reach 1000, the system remains stable and serves over 94% of its intended traffic, though the increase in redirected aircraft is 56 per day, indicating this as the maximum efficient capacity, approaching a capacity limit.

A critical breaking point is observed at 1200 arrivals per day. Here, the service rate drops sharply to 84.53%, and redirections jump to an average of 185 per day, a nearly 230% increase in redirections for only a 20% increase in demand. By exceeding the 85% utilization threshold, the vertiport leads to a breakdown in operational reliability and a significant increase in flight diversions. This is a common limit used by the International Civil Aviation Organization (ICAO) [33].

As demand scales past 2500, the vertiport enters a state of total saturation. Despite demand doubling or tripling, the actual number of eVTOLs served ($\mathcal{N}_{\text{eVTOL}}$) plateaus at 1500–2000, indicating the absolute physical limit of the resources. At extreme demand (10,000+ arrivals), the overall throughput collapses to below 0.45, and the system redirects four times as many aircraft as it serves. These results confirm that, for this specific vertiport configuration, demand exceeding 1200 arrivals per day requires either resource expansion or strict slot management.

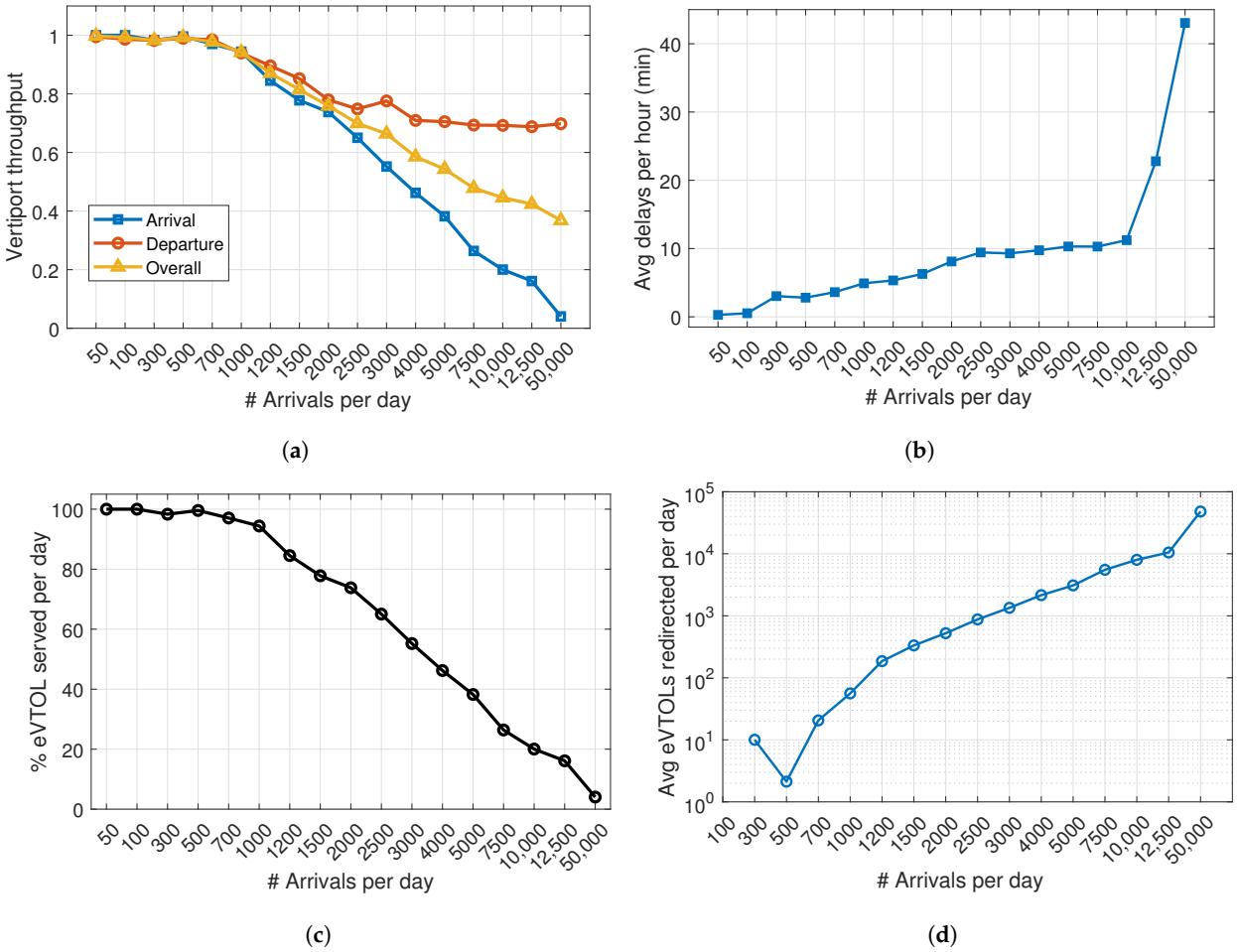

Figure 10. Relationship between arrival demand and vertiport performance across 100 iterations based on defined metrics. The X-axis shows the number of arrivals per day (#Arrivals) and the Y-axis gives the (**a**) vertiport throughput; (**b**) average delays per hour; (**c**) the percentage of eVTOLs served per day and; (**d**) average number of eVTOLs redirected.

7. Conclusions

This paper addresses the challenges of managing vertiport capacity and throughput using a proposed dual-level taxiing and parking architecture. A dynamic scheduling approach was proposed to maximise efficiency by arranging eVTOL arrivals and departures. The solution strategy also integrated eVTOL battery charging and parking into the operational flow. Monte Carlo simulations of up to 50,000 operations were used to measure reliability and throughput, thereby identifying the precise point at which the system transitions from stable to congested. The results demonstrate that the vertiport operates at peak efficiency up to 1000 arrivals per day, maintaining an overall throughput of 94% with minimal delays. However, the critical breaking point occurs at 1200 arrivals per day, at which the service rate reaches 84.5% and the overall throughput is 87%. Delays increased significantly beyond the arrival demand of 1200 per day, resulting in increased eVTOL redirections. Hence, the maximum capacity of the vertiport was found to be 1200 arrivals per day to maintain high-quality service.

Future work in this area includes expanding the current study by testing various vertiport configurations at two levels and incorporating additional scenarios, such as the effects of flight cancellations or emergency situations. A realistic demand scenario

incorporating peak and non-peak hours for different vertiport configurations and resources to find their breaking points could also be studied.

Author Contributions: Conceptualization, S.R.N. and T.J.L.; methodology, S.R.N.; software, S.R.N.; validation, S.R.N.; formal analysis, S.R.N.; investigation, S.R.N.; resources, S.R.N.; data curation, S.R.N.; writing—original draft preparation, S.R.N. and T.J.L.; writing—review and editing, S.R.N. All authors have read and agreed to the published version of the manuscript.

Funding: This research received no external funding.

Data Availability Statement: The source code used could not be shared.

Conflicts of Interest: The authors declare no conflicts of interest.

References

1. United Nations. *Policies on Spatial Distribution and Urbanization Have Broad Impacts on Sustainable Development*; Department of Economic and Social Affairs: New York, NY, USA, 2020.
2. FAA. Urban Air Mobility (UAM) concept of operations. *NextGen Off.* **2023**, *2*, 33.
3. National Aeronautics and Space Administration (NASA) Advanced air mobility: What is AAM? *Stud. Guide* **2020**, *5*, 1–6.
4. European Commission. A Drone Strategy 2.0 for a Smart and Sustainable Unmanned Aircraft Eco-System in Europe. *Air Space Law* **2023**, *48*, 273–296.
5. Andritsos, K.; Scott, B.I.; Trimarchi, A. What is in a name: Defining key terms in urban air mobility. *J. Intell. Robot. Syst.* **2022**, *105*, 81. https://doi.org/10.1007/s10846-022-01694-1.
6. Plötner, K.; Straubinger, A.; Preis, L.; Shamiyeh, M. Putting Urban Air Mobility into Perspective. *Bauhaus-Luftfahrt-Aviation Think Tank* **2022**, *Whitepaper*, 1–12. Available online: https://www.bauhaus-luftfahrt.net/fileadmin/user_upload/News/Whitepaper/UAM_White_Paper_2022.pdf (accessed on 7 December 2025).
7. Bauhaus Luftfahrt. Market Potential of Aircraft for Urban and Regional Air Mobility. *The Aviation Think Tank*, 2024. Available online: www.bauhaus-luftfahrt.net/en/research-areas/urban-regional-air-mobility/market-potential-of-air-vehicles-for-urban-and-regional-air-mobility (accessed on 7 December 2025).
8. Carroll, R. We Really, Really Need Vertiports—A Successful Take-off Begins on the Ground. *Airframe*, 2023. Available online: https://airframe.substack.com/p/we-really-really-need-vertiports (accessed on 7 December 2025).
9. Preis, L.; Hornung, M. Vertiport operations modelling, agent-based simulation and parameter value specification. *Electronics* **2022**, *11*, 1071. https://doi.org/10.3390/electronics11071071.
10. European Union Aviation Safety Agency (EASA) *Vertiports in the Urban Environment*; EASA: Cologne, Germany, 2022.
11. European Union Aviation Safety Agency (EASA). *Special Condition Vertical Take-Off and Landing (VTOL) Aircraft*; EASA: Cologne, Germany, 2021; pp. 1–31.
12. European Union Aviation Safety Agency (EASA) *Vertiports Prototype Technical Specifications for the Design of VFR Vertiports for Operation with Manned VTOL-Capable Aircraft Certified in the Enhanced Category (PTS-VPT-DSN)*; EASA: Cologne, Germany, 2021; pp. 1–179.
13. Sievers, T.F.; Geister, D.; Schwoch, G.; Peinecke, N.; Schuchardt, B.I.; Volkert, A.; Lieb, T.J. Initial conops of U-space flight rules (UFR). *DLR Bluepr.* **2024**, *1*, 1–39.
14. Brunelli, M.; Ditta, C.C.; Postorino, M.N. New infrastructures for Urban Air Mobility systems: A systematic review on vertiport location and capacity. *J. Air Transp. Manag.* **2023**, *112*, 102460. https://doi.org/10.1016/j.jairtraman.2023.102460.
15. Preis, L.; Hornung, M. A vertiport design heuristic to ensure efficient ground operations for urban air mobility. *Appl. Sci.* **2022**, *12*, 7260. https://doi.org/10.3390/app12147260.
16. Schweiger, K.; Preis, L. Urban Air Mobility: Systematic review of scientific publications and regulations for vertiport design and operations. *Drones* **2022**, *6*, 179. https://doi.org/10.3390/drones6070179.
17. Straubinger, A.; Rothfeld, R.; Shamiyeh, M.; Büchter, K.D.; Kaiser, J.; Plötner, K.O. An overview of current research and developments in urban air mobility—Setting the scene for UAM introduction. *J. Air Transp. Manag.* **2020**, *87*, 101852. https://doi.org/10.1016/j.jairtraman.2020.101852.
18. Rimjha, M.; Trani, A. Urban Air Mobility: Factors affecting vertiport capacity. In *Proceedings of the 2021 Integrated Communications Navigation and Surveillance Conference (ICNS)*; IEEE: Dulles, VA, USA, 2021; pp. 1–14. https://doi.org/10.1109/ICNS52807.2021.9441631.
19. Guerreiro, N.M.; Hagen, G.E.; Maddalon, J.M.; Butler, R.W. Capacity and throughput of urban air mobility vertiports with a first-come, first-served vertiport scheduling algorithm. In Proceedings of the AIAA Aviation 2020 Forum, Online, 8 June 2020; p. 2903. https://doi.org/10.2514/6.2020-2903.

20. Schuchardt, B.I.; Geister, D.; Lüken, T.; Knabe, F.; Metz, I.C.; Peinecke, N.; Schweiger, K. Air Traffic Management as a vital part of Urban Air Mobility—A review of DLR's research work from 1995 to 2022. *Aerospace* **2023**, *10*, 81.
21. Schuchardt, B.I.; Devta, A.; Volkert, A. Integrating vertidrome management task into U-space. *arXiv* **2023**, arXiv:2309.09584. https://doi.org/10.48550/arXiv.2309.09584.
22. Schweiger, K.; Knabe, F. Vertidrome airside level of service: Performance-based evaluation of vertiport airside operations. *Drones* **2023**, *7*, 671. https://doi.org/10.3390/drones7110671.
23. Preis, L.; Vazque, M.H. Vertiport throughput capacity under constraints caused by vehicle design, regulations and operations. In Proceedings of the Delft International Conference on Urban Air-Mobility (DICUAM), Delft, The Netherlands, 22–24 March 2022; pp. 1–12.
24. Curlander, J.C.; Gilboa-Amir, A.; Kisser, L.M.; Koch, R.A.; Welsh, R.D. Multi-Level Fulfillment Center for Unmanned Aerial Vehicles, 2017. US Patent US9777502B2, 3 October 2017.
25. Vascik, P.D.; Hansman, R.J. Development of vertiport capacity envelopes and analysis of their sensitivity to topological and operational factors. In Proceedings of the AIAA Scitech 2019 Forum, San Diego, CA, USA, 7–11 January 2019; p. 0526. https://doi.org/10.2514/6.2019-0526.
26. Preis, L. Quick sizing, throughput estimating and layout planning for VTOL aerodromes—A methodology for vertiport design. In Proceedings of the AIAA Aviation 2021 Forum, Virtual, 2–6 August 2021; p. 2372. https://doi.org/10.2514/6.2021-2372.
27. Yang, X.G.; Liu, T.; Ge, S.; Rountree, E.; Wang, C.Y. Challenges and key requirements of batteries for electric vertical Take-Off and landing aircraft. *Joule* **2021**, *5*, 1644–1659. https://doi.org/10.1016/j.joule.2021.05.001.
28. EUROCONTROL. *CORUS-XUAM—U-space concept of operation (ConOps)*; SESAR Joint Undertaking: Brussels, Belgium, 2023; Grant ID 101017682, pp. 1–1168. https://doi.org/10.2829/207917.
29. European Commission. EUREKA—European key solutions for vertiports and UAM. *SESAR Joint Undertaking* 2023. Available online: https://milanairports.com/en/sustainability/all-sea-projects/eureka-european-key-solutions-vertiports-and-uam (accessed on 7 December 2025).
30. Schwartz, C.W.; Witczak, M.W.; Leahy, R.B. *Structural Design Guidelines for Heliports*; Systems Control Technology, Inc. No. DOTFAAPM8423; Florida, 24 October 1984. Available online: https://apps.dtic.mil/sti/tr/pdf/ADA148967.pdf (accessed on 7 December 2025).
31. Hagag, N.; Gasche, S.; Jäger, F.; Kallies, C. Energy Demand Analysis for eVTOLs in Cluttered and Dynamic Environments based on Adaptive Trajectory Prediction. In *Proceedings of the 2024 Integrated Communications, Navigation and Surveillance Conference (ICNS)*; IEEE: Herndon, VA, USA, 2024; pp. 1–15. https://doi.org/10.1109/ICNS60906.2024.10550722.
32. Nagrare, S.R.; Ghose, D. Dronecage: A model for conflict resolution in aerial corridor intersections. *J. Aerosp. Inf. Syst.* **2025**, *22*, 202–219. https://doi.org/10.2514/1.I011473.
33. International Civil Aviation Authority (ICAO). 9971 Manual on Collaborative Air Traffic Flow Management. Quebec, Canada, 2012. Available online: https://store.icao.int/en/manual-on-collaborative-air-traffic-flow-management-doc-9971 (accessed on 7 December 2025).

Disclaimer/Publisher's Note: The statements, opinions and data contained in all publications are solely those of the individual author(s) and contributor(s) and not of MDPI and/or the editor(s). MDPI and/or the editor(s) disclaim responsibility for any injury to people or property resulting from any ideas, methods, instructions or products referred to in the content.